Russian Journal of Earth Sciences

Geophysical Imaging of the Crust for the Source Area of the Khastakh Earthquake (NE Margin of the Siberian Platform, Yakutia)

A. S. Kulyandina[1*], A. I. Filippova[2], and E. Yu. Sokolova[3,4]

[1] Yakutsk Branch of Federal Research Center, Geophysical Survey of RAS, Yakutsk, Russian Federation
[2] Pushkov Institute of Terrestrial Magnetism, Ionosphere and Radio Wave Propagation of RAS, Moscow, Troitsk, Russian Federation
[3] All-Russian Research Geological Oil Institute, Moscow, Russian Federation
[4] Schmidt Institute of Physics of the Earth of RAS, Moscow, Russian Federation
* **Correspondence to:** Albina Kulyandina, albineku@gmail.com

Abstract: In this study, we focus on the crustal structure in the vicinity of the source area of the May 20, 2011 Khastakh earthquake with $M_w = 4.7$. An interest in this seismic event is connected with a fact that it occurred within the Lena-Anabar trough at the margin of the Siberian platform, which is characterized by very low level of seismic activity. Spatial characteristics of the gravity and magnetic fields were studied and 3D models of the crustal density and magnetization contrasts were constructed using data on gravity and magnetic surveys and GIS INTEGRO software. A network of buried faults, to one of which the Khastakh earthquake is related, has been revealed. The presence of a magmatic intrusion, probably, playing a role in the redistribution of the crustal stress-strain state in the vicinity of the considered seismic event, is suggested based on the constructed crustal 3D models. The obtained results regarding structural frames of the Khastakh earthquake source were verified by previous magnetotelluric and seismic studies.

Keywords: gravity and magnetic fields, Khastakh earthquake, Siberian platform, GIS INTEGRO.

Citation: Kulyandina A. S., Filippova A. I., and Sokolova E. Yu. (2025), Geophysical Imaging of the Crust for the Source Area of the Khastakh Earthquake (NE Margin of the Siberian Platform, Yakutia), *Russian Journal of Earth Sciences*, 25, ES4008, EDN: CJVEYI, https://doi.org/10.2205/2025es001004

Introduction

The Siberian platform is characterized by a low level of seismic activity. Rare and weak earthquakes occur within its territory, primarily, concentrating along the platform margins [*Imaeva et al.*, 2021; *Radziminovich and Shchetnikov*, 2008; *Seminskii and Radziminovich*, 2007; *Seredkina et al.*, 2015]. The northeastern margin of the Siberian platform is not an exception – only few seismic events with $M < 5$ were registered there during the whole period of instrumental observations (since 1963) (Figure 1). Therefore, such events are of special interest. The strongest of them is the May 20, 2011 Khastakh earthquake with $M_w = 4.7$ [*Seredkina and Melnikova*, 2018]. According to the data of the Yakutsk Branch of FRC GS RAS (https://yakgsras.ru/), its epicenter is located within the Khastakh graben-rift of the Lena-Anabar trough, in the relative proximity of the Olenek bitumen field [*Khudoley et al.*, 2022] (Figure 1). Uncertainties of the earthquake epicenter are about 2 km in longitude and 9 km in latitude. Five foreshocks with $M < 5.0$ ($K_p = 7.9$–10.3) were detected during 4 days before the mainshock which was followed by only one weak aftershock ($K_p = 8.3$) (https://yakgsras.ru/). A source depth of 3 km, scalar seismic moment of 1.3×10^{16} N m and focal mechanism of the Khastakh earthquake were determined in [*Seredkina and Melnikova*, 2018] from intermediate-period surface wave amplitude spectra using a method by *Bukchin* [1990]. These source parameters are characterized by low residual values (0.218) and, therefore, can be regarded as reliable. Resolution of the obtained depth is good as a partial residual function has a sharp minimum [*Seredkina and Melnikova*, 2018, Fig. 6c]. The depth uncertainty, estimated as a depth range in which the partial residual function varies by 10% of its minimum, is about 2 km.

Research Article

Received: November 29, 2024
Accepted: February 21, 2025
Published: July 30, 2025

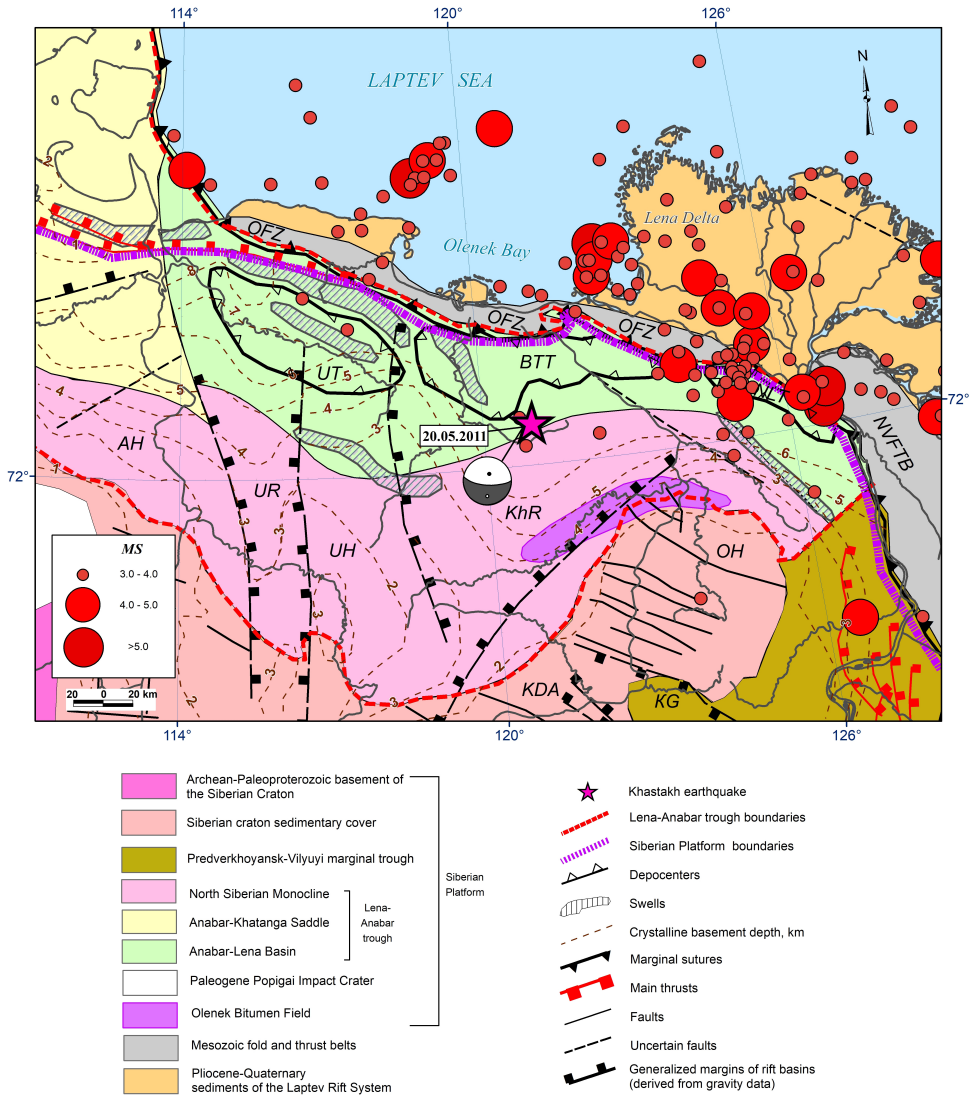

Figure 1. Tectonic map of the Lena-Anabar trough and adjacent areas according to [*Khudoley et al.*, 2022] with the following abbreviations: AH, Anabar High; BTT, Buolkalakh–Taimylyr Trough; KhR, Khastakh Rift; KDA, Kuoisk–Daldynsk Arch; KG, Kyutingda Graben; NLT, Nizhne–Lena Trough; NVFTB, North Verkhoyansk Fold and Thrust Belt; OFZ, Olenek Fold Zone; OH, Olenek High; UH, Udzha High; UR, Udzha Rift; UT, Uyelin Trough. Epicenters of regional earthquakes ($M \geq 3.0$, 1963–2022) are plotted according to the catalog by the Yakutsk Branch of FRC GS RAS (https://yakgsras.ru/). Magnitudes were recalculated from energy classes using a relation from [*Rautian et al.*, 2007]. The focal mechanism of the May 20, 2011 Khastakh earthquake with $M_w = 4.7$ is plotted in a lower hemisphere projection according to [*Seredkina and Melnikova*, 2018].

The main objective of the current study was to reveal the features of the deep crustal structure which specify the position of the source area of the Khastakh earthquake. According to the experience of our recent research [*Kulyandina et al.*, 2024] and many other studies [*Dong et al.*, 2022; *Kim et al.*, 2022; *Yang et al.*, 2023; *Zhang et al.*, 2010, etc.], to achieve this goal, an integrated analysis of geophysical fields of different nature has been chosen as the most productive approach. The extensive geophysical datasets, collected during a regional stage of oil and gas prospecting in the Lena-Anabar trough, were used [*Chenborisova*, 2016a,b]. With applying modern GIS-technologies (the GIS INTEGRO software developed in VNIGNI [*Cheremisina et al.*, 2021], a variety of morphological/statistical parameters

of geopotential fields' spatial distribution [compiled in *Buzikova et al.*, 2004; and *Lisnik*, 2006] as well as their modeling results were examined. Thus, for the clarification of the seismotectonic pattern in the area of the Khastakh earthquake, 3D models of the crustal density and magnetization contrasts were constructed and compared with the results of previous 3D magnetotelluric field inversion [*Slinchuk et al.*, 2022] and the nearest reflection seismic cross-sections [*Kontorovich et al.*, 2013].

Data and Methods

To better understand the factors, controlling the development of the Khastakh earthquake source area, as well as to identify potential sites of new seismic events in the considered zone of the Lena-Anabar trough, we analyzed geophysical images of deep crustal structures in a certain volume around the earthquake location, which reflect the corresponding inhomogeneities in the distribution of physical properties of rocks, namely, density and magnetization. To study the morphology of anomalous geopotential fields, as well as to conduct their 3D inversions, data from regional gravimetry [*Buzikova et al.*, 2004] and magnetic surveys [*Lisnik*, 2006] (Figure 2) were used with the GIS INTEGRO software package being applied as a toolkit [*Cheremisina et al.*, 2021]. The gravity field data are results of regional gravimetric surveys at a scale of 1:200,000, carried out mainly on a grid of (3×3)–(2×3) km (an error in measuring the anomaly values is 0.5–1 mGal) [*Buzikova et al.*, 2004]. Magnetic field anomalies are results of regional geomagnetic surveys at a scale of 1:200,000 carried out at an altitude of 200 m with a fluxgate aerial magnetometer AEM-49 (analog field recording division value of 3.5 nT/mm, nonlinear zero drift of up to 30 nT/hour, and temperature coefficient of 8 nT/1 °C) [*Lisnik*, 2006]. The selected program tool combines the capabilities of a geoinformation system to spatially compare heterogeneous geological and geophysical information in order to carry out its integrated interpretation, offers a wide range of procedures for morphological and statistical analysis of geophysical fields, as well as for geophysical modeling and inversions in grid models of various dimensions.

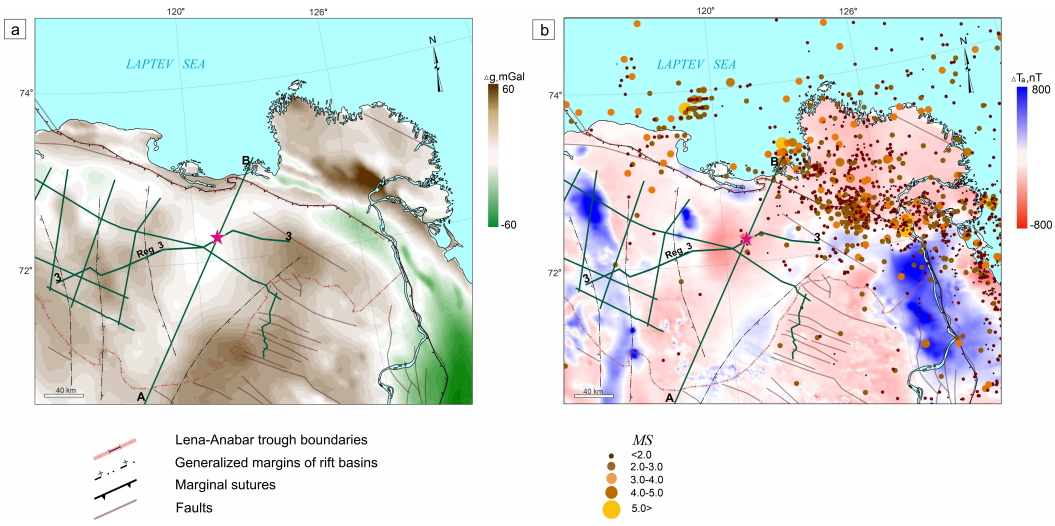

Figure 2. Distribution of the geopotential fields over the area under study: the map of gravity field (Bouguer anomalies, intermediate layer density is 2.67 g/cm^3) (a) [*Buzikova et al.*, 2004] and the magnetic anomaly map (b) [*Lisnik*, 2006]. Tectonic lines are plotted according to Figure 1. Regional seismicity according to the catalog by the Yakutsk Branch of FRC GS RAS (https://yakgsras.ru/) is superimposed on panel (b). The regional prospecting geophysical profiles are shown as dark green lines: AB – the line of the cross-section in Figures 4 and 5. The line of the composite seismic profile (Reg_3) in Figure 7 is marked as 3–3′. The epicenter of the Khastakh earthquake is marked by a violet star.

In our previous study [*Kulyandina et al.*, 2024], the technologies of GIS INTEGRO have already allowed us to trace the main features of the spatial character and calculated statistical parameters of the gravity and magnetic fields within the Lena-Anabar trough, and to compare them with regional seismicity for establishing correlations of potential fields' anomalies with regularities in the distribution of earthquake epicenters. To support the obtained results and to characterize in more details the Khastakh earthquake source area, at which we concentrate in the current research, an additional informative transformation of the gravity field was reviewed – namely, the coefficient of the asymmetry in the field distribution (Figure 3a). This dimensionless parameter Skew (skewness) is estimated in the sliding square window (in particular, of 10×10 km size with 50% spatial overlapping) over the area under interest according to the known determination:

$$\text{Skew} = \frac{\sum_{i=1}^{n} (x_i - \overline{x})^3}{n} \frac{1}{\sigma^3},$$

where x_i, $i = 1, n$ are grid values of the field in each square window and $\overline{x} = \sum_{i=1}^{n} (x_i)/n$ is a corresponding arithmetic mean, and $\sigma = \sum_{i=1}^{n} (x_i - \overline{x})^2/n$ is a dispersion.

This characteristic is effective in highlighting linear gradient zones of the geopotential fields, which are marked by a transition from positive to negative Skew-values (from a left-skewed statistical distribution of grid values of the field in a window to a right-skewed one). The analysis of the asymmetry parameter of the gravity field compliments the results of the detection of the local linear anomalies in the magnetic field (example according to [*Kulyandina et al.*, 2024] is presented in Figure 3b) in terms of providing well-distinguished images of elongated crustal structures with material properties contrasting with the host environment (faults, dykes, etc.).

Volume distributions of density and magnetization contrasts in the area of the Lena-Anabar trough, embracing the Khastakh earthquake source zone, were also recovered using GIS INTEGRO, in which procedures of spectral 3D inversions of the potential fields have been realized [*Mitsyn*, 2018] based on developments by [*Kobrunov and Varfolomeev*, 1981; *Priezzhev*, 1989]. In this approach, the solution of the inverse problem of gravity and magnetic fields is delivered via the following formalism in a spatial wavenumber domain (according to [*Priezzhev et al.*, 2014]):

$$D(\omega_1, \omega_2, z) = \frac{1}{\gamma} G(\omega_1, \omega_2, 0) \frac{K(\omega_1, \omega_2, z)}{\int_{z'=0}^{\infty} K(\omega_1, \omega_2, z') e^{-rz'} dz'},$$

where $D(\omega_1, \omega_2, z)$ is a density spectrum at depth z, $G(\omega_1, \omega_2, 0)$ is a spectrum of the observed gravity/magnetic field, $K(\omega_1, \omega_2, z)$ is a function describing the density spectrum dependence on depth (z), ω_1 and ω_2 are spatial wavenumbers corresponding to horizontal coordinates x and y, respectively, $r = \sqrt{\omega_1^2 + \omega_2^2}$ is a radial wavenumber, γ is the gravity constant. The equivalence of the solutions of the ill-posed inverse geophysical problem (non-uniqueness) is reflected in a wide variability of possible kinds of K-dependences, arbitrary in a general case. The parameters of the procedure of the inverse problem solution, responsible for the choice of this dependence, are usually set in accordance with preliminary regional experience or constraints from other geophysical data.

In our case, the iterating through the parameters and their final selection were realized via comparison of the variety of the resulting density/magnetization perturbations (local anomalies) with the images of the deep structure features available from the data of profile seismic and magnetotelluric soundings [*Chenborisova*, 2016b; *Kontorovich et al.*, 2013; *Slinchuk et al.*, 2022] (Figure 2a). The current cube of 3D distributions of density or magnetization contrasts were cut into vertical slices along the lines of the prospecting profiles and corresponding anomalous features in the different cross-sections were compared iteratively up to achieving the appropriate convergence in their depth characteristics. Installations of cross-sections of the finally chosen solutions for the magnetic and gravity fields are shown in Figures 4 and 5.

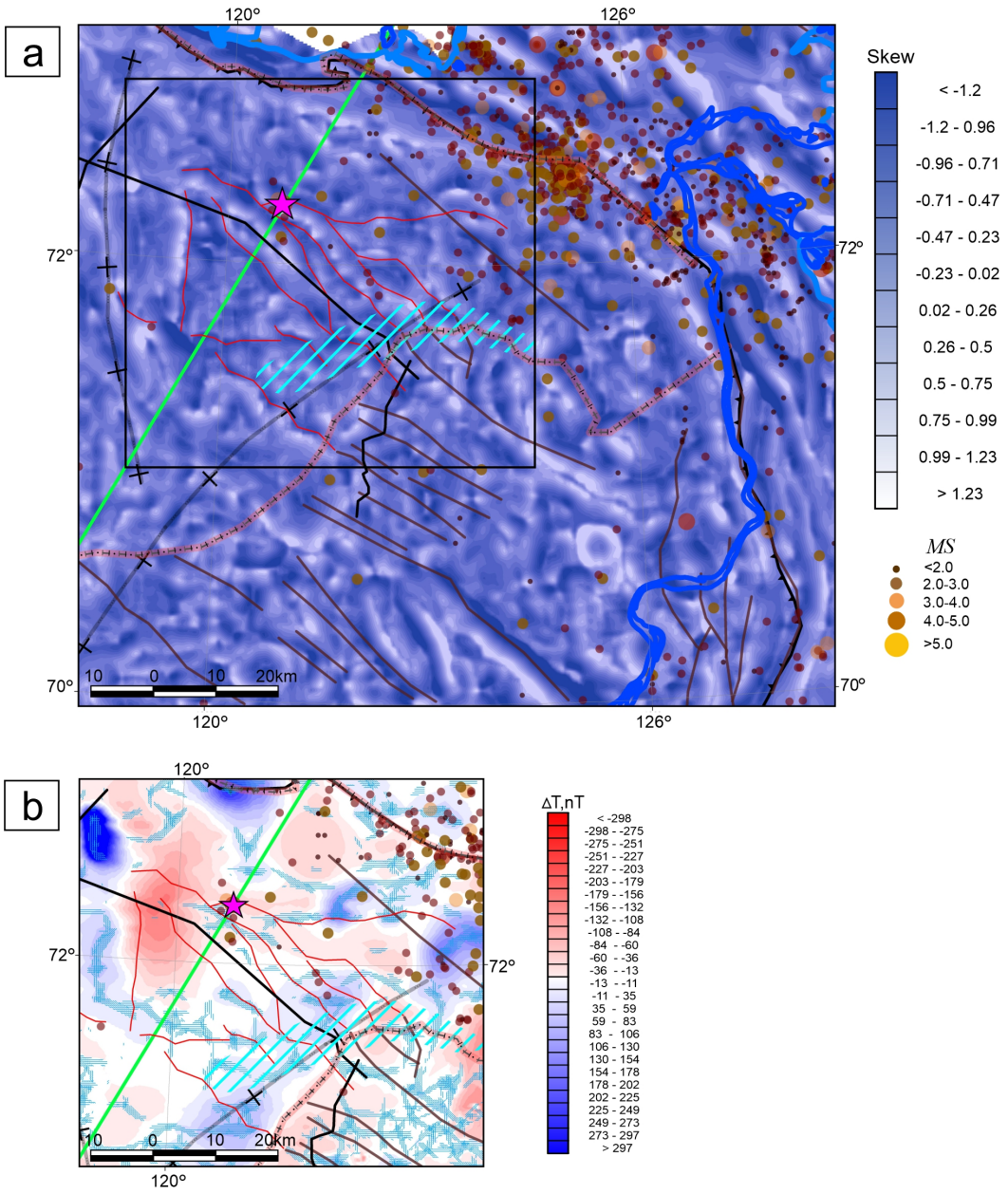

Figure 3. The distribution of the asymmetry parameter of the local gravity anomalies (in part of the unit) (a) and the results of the detection of the linear positive magnetic anomalies (according to [*Kulyandina et al.*, 2024] on the background of the map of the local component of the lithospheric magnetic field (in nT) (b). Brown lines – known faults. The red lines – inferred faults in the area of Khastakh earthquake. Turquoise hatching marks the Olenek bitumen field. The remaining symbols are shown in the legends to Figures 1 and 2. Black rectangle in panel (a) marks the area shown in panel (b). The epicenter of the Khastakh earthquake is marked by a violet star.

Results and Discussion

Our analysis of the potential fields' spatial morphology, based on a traditional postulate of a conservative inheritance of the lineaments of the field on tectonic structures, was aimed at imaging a fault network pattern, which could be related to the Khastakh earthquake development.

Areal distribution of the skewness parameter, demonstrated in Figure 3, is characterized by linear structures with a regular conversion from positive to negative Skew-values

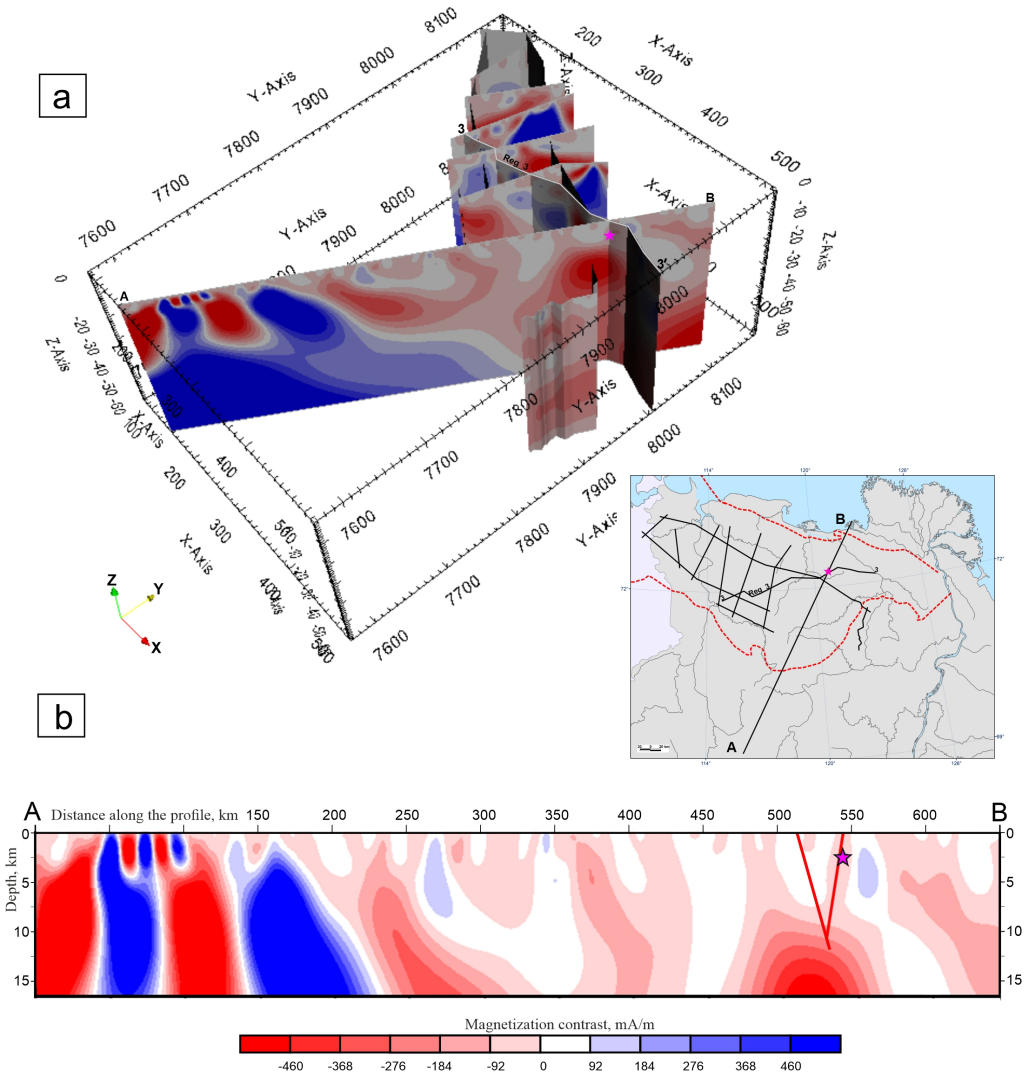

Figure 4. Spatial installation of the vertical sections of a 3D model of magnetization contrast along the set of geophysical profiles (a) and cross-section of this model along the line AB passing through the epicenter of the Khastakh earthquake. The Khastakh earthquake source location according to [*Seredkina and Melnikova*, 2018] is given as a violet star and inferred faults – as red lines. Color axis direction: *X* – East, *Y* – North, *Z* – depth. Inserted map demonstrates position of the cross-section lines.

(generally, reflecting a transition of the dominance of small field values to big ones). These Skew-disturbances of different intensity mark the corresponding depth-spatial variations in density which may be associated with boundaries of various crustal blocks ("step-wise" anomalies) or linear structures with local density contrasts. Whether the latter belong to weakened or, conversely, "healed" by heavy magmatic material (dikes) fault zones should be reflected in the spatial order of Skew-changes, but cannot be distinguished in the Skew-distribution without additional information. The known large faults in the considered region (the largest faults at the Olenek High, faults along the Kyutingda graben sides and at the frontal zone of the North Verkhoyansk Fold and Thrust Belt (NVTB)) are marked by similar bright linear anomalies in the Skew-distribution (Figures 3a and 1). According to the patterns of these images (following the lines of Skew-transition from negative to positive values), we have inferred a network of faults around the Khastakh earthquake epicentral area (Figure 3a), which were not revealed by geologists earlier because of the thick Mz sedimentary cover in the graben [*Khudoley et al.*, 2022]. A general strike of the majority of the inferred faults corresponds well to the NW pattern of the regional fault

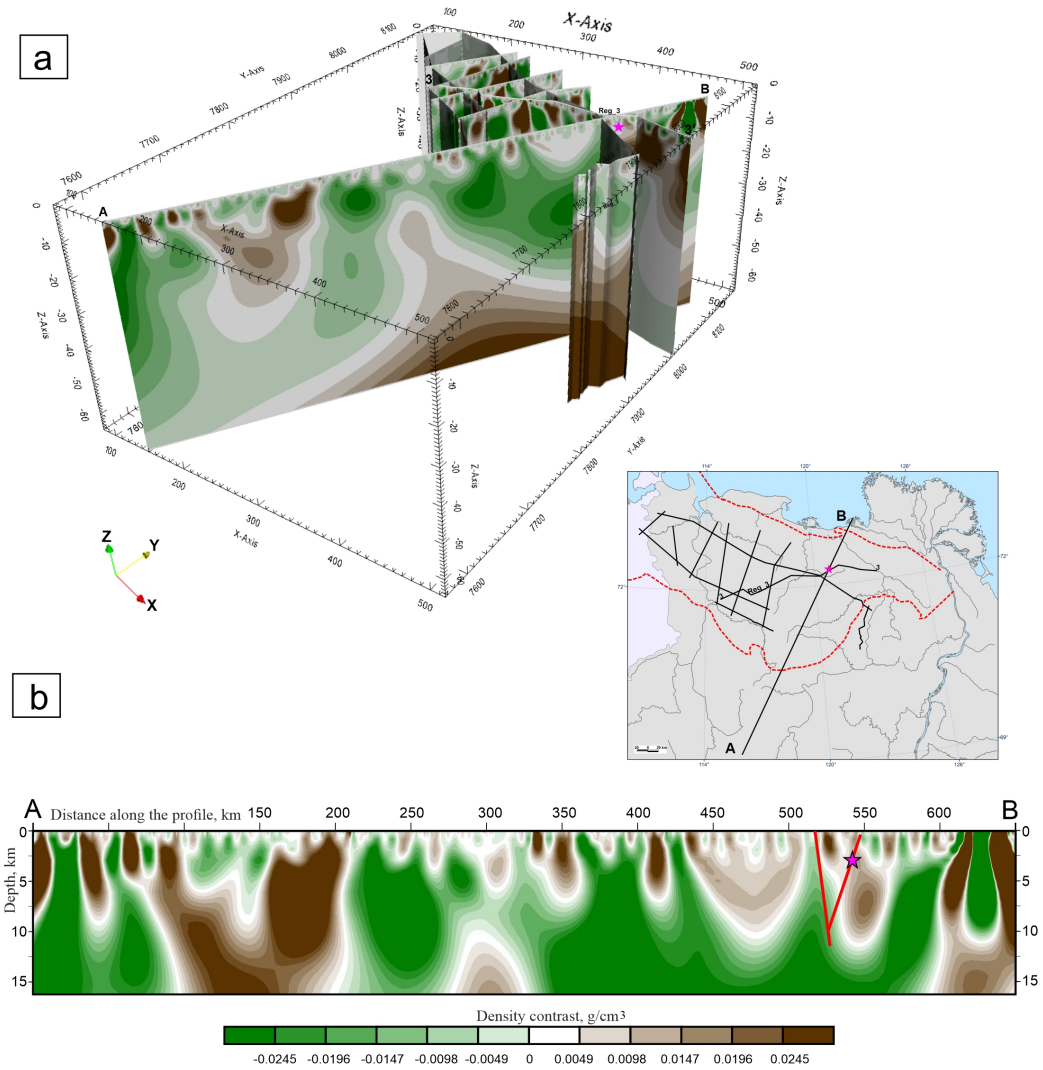

Figure 5. Spatial installation of the vertical sections of a 3D model of density contrast along the set of geophysical profiles (a) and cross-section of this model along the line AB passing through the epicenter of the Khastakh earthquake (b). The Khastakh earthquake source location is given as a violet star and inferred fault – as red lines. Color axes and profile line locations are the same as those in Figures 2 and 4.

system, with some of them being continuations of the known faults at the Olenek High. Several of these buried disjunctives correspond to elements of a pattern of local magnetic anomalies which have been highlighted by their axial lines in [*Kulyandina et al.*, 2024] and are now replicated in Figure 3b. They probably represent the fault zone with mineralization development or filled with magmatic material. Several weak instrumentally registered seismic events are likely related to the revealed fault structures (Figure 3a). The epicenter of the Khastakh earthquake, the most strong event within the considered region, has appeared to be coincident with the cross of disjunctive structures stretching in sub-latitudinal and NW directions. It is worth noting that the focal mechanism of this earthquake was determined in [*Seredkina and Melnikova*, 2018] as a normal fault with nodal planes oriented also in sub-latitudinal directions (strike angles are 105° and 295°) (Figure 1).

The assumption of the Khastakh earthquake source development in the fault plane of the sub-latitudinal strike is supported by the analysis of the results of the 3D spectral inversions of the gravity and magnetic fields. Figures 4 and 5 show the resulting models of density and magnetization contrasts and present the spatial installations of the model cross-

sections along the network of the regional geophysical prospecting profiles [*Chenborisova*, 2016a,b], Reg_3 profile line [from *Kontorovich et al.*, 2013], as well as an additional section along the line AB, passing through the Khastakh earthquake with the source location [according to *Seredkina and Melnikova*, 2018] being marked by a star. Ideas on the SW-dipping fault plane can be inferred from the analysis of the density and magnetization modeled sections across the hypocenter (Figures 4b and 5b). They are additionally supported by the fact that one of the nodal planes, determined from surface wave inversion (Figure 1), is characterized by steep SW-dipping (a dip angle is 75°) [*Seredkina and Melnikova*, 2018]. Therefore, based on strikes and dip of the inferred faults (Figures 3, 4 and 5), we can suggest this nodal plane to be a rupture plane. The obtained images also confirm a concept of the presence in the neighborehood of the earthquake source of a magmatic intrusion, probably, fed by this magma-controlling fault. The intrusive body is located at the depths of 6–8 km and characterized by a positive density contrast and enhanced magnetic properties at its top.

Obtained from the analysis of the potential fields assumptions about the seismotectonic pattern, associated with the Khastakh seismic event, were verified with geoelectric modeling results: data of prospecting MTS profiling as well as results of regional 3D resistivity modeling performed in [*Slinchuk et al.*, 2022]. Figure 6a demonstrates the projection of the Khastakh earthquake source [according to *Seredkina and Melnikova*, 2018] on the geoelectric section along the nearest MTS profile [*Chenborisova*, 2016b], where it is attributed to the area of contrasting electrical resistivity pattern. This resistivity contrast, probably, corresponds to the base of the resistive Paleozoic carbonates overlapping the conducting Riphean terrigenous and fluidized sedimentary infill of the Khastakh graben. It is also worth noting that in this resistivity cross-section one can clearly distinguish images of three faults, which correspond to similar structures inferred from the spatial distribution of the Skew-parameter of the gravity field and presented in a planar view in Figures 3 and 6b. Figure 6b shows the horizontal slice of volume geoelectric model at 3-km depth which is correspondent to the earthquake source. This figure demonstrates that the seismic event was formed in the zone of lateral contact of resistive and conductive zones. The entire adjacent area of increased conductivity is enclosed between faults identified based on the analysis of potential fields and can be confidently interpreted as an area composed by terrigenous sediments of enhanced fluidization, and so – as rheologically weak one.

The additional understanding of the seismotectonic features responsible for the Khastakh earthquake comes from the revision of the reflection seismic section along the profile Reg_3 from [*Kontorovich et al.*, 2013], where the location of the source corresponds to the anomalous disturbance of the reflection horizons and the variations in the character of the reflectivity pattern which could be produced by faulting and injection of magmatic material (Figure 7).

Finally, we compared the obtained results with crustal features revealed in previous studies of weak and strong seismic events occurred in different regions of the Earth. In terms of seismic wave velocities, earthquakes are commonly related to zones with a sharp contrast of P- and S-wave velocities [*Arefiev et al.*, 2006; *Kayal et al.*, 2002; *Wei and Zhao*, 2016] that is also realized in the Eastern Siberia, for example, in the source area of the January 17, 2014, earthquake (M_w = 4.3) in the south of the Siberian platform [*Seredkina et al.*, 2015]. In many cases the correlation of such zones with areas of significant variations of the Poisson's ratio [*Gou et al.*, 2020; *Krylov and Ten*, 1995] and attenuation (i.e., rheological properties) [*Kopnichev and Sokolova*, 2003] is additionally determined. The aforementioned areas of enhanced seismicity and seismic velocity peculiarities are frequently found in the nearest neighborhood with the areas of crustal conductivity contrasts [*Sokolova et al.*, 2007; *Sokolova et al.*, 2016; *Unsworth*, 2009]. In terms of the gravity field, fault zones, in which seismic events are concentrated, are often marked by gradients of gravity anomalies [*Kim et al.*, 2022; *Wu et al.*, 2015; *Yang et al.*, 2023; *Zhang et al.*, 2010] as we have previously emphasized for the Lena-Anabar suture [*Kulyandina et al.*, 2024] and confirmed in this study. Magnetic field features, traced in the epicentral areas of strong and moderate

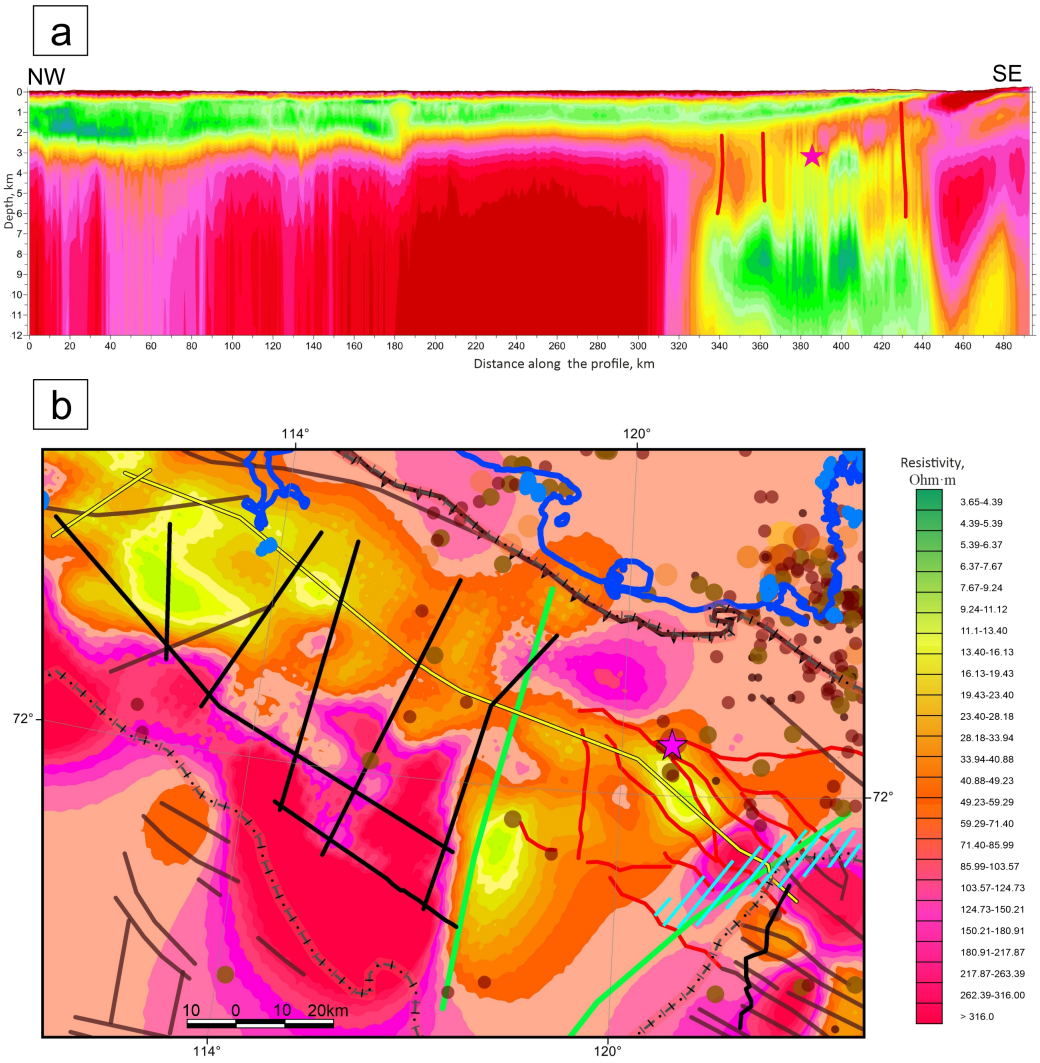

Figure 6. Spatial localization of the Khastakh earthquake source (violet star), projected on a 1D geoelectric section along the composite MTS profile [*Chenborisova*, 2016b] (a) and on the horizontal slice of a volume geoelectric model (3D MT inversion results [*Slinchuk et al.*, 2022]) at the depth of 3 km (b). In panel (b): prospecting regional MTS and CDP profiles are shown as black lines, with yellow one indicating the line of section presented in panel (a). Known faults are shown as brown lines, Khastakh rift borders – green lines [according to potential fields' analysis in *Kulyandina et al.*, 2024], inferred fault lines in (a) and (b) – red lines (according to the analysis of the resistivity cross-section and the gravity field Skew-parameter distribution in Figure 3). The remaining symbols are shown in the legends to Figures 1 and 2.

earthquakes, are more controversial. In some cases, strong seismic events are observed within strong negative magnetic anomalies [*Wu et al.*, 2015; *Zhang et al.*, 2010] while in the others, they are nucleated within both strong positive and negative magnetic anomalies even within a single region with a relatively uniform seismotectonic pattern [*Yang et al.*, 2023]. Magnetic anomaly gradients [*Kim et al.*, 2022] and abrupt changes in the bottom depth of lithospheric magnetic sources [*Filippova and Filippov*, 2024; *Wen et al.*, 2021] could also accommodate strong seismicity. As far as moderate earthquakes are concerned, they are comprised to the areas with weak magnetic anomalies of both signs and their boundary zones [*Dong et al.*, 2022], which are probably correspondent to the magmatic injections or mark mineralized fault zones that is consistent with our results (Figures 3 and 4).

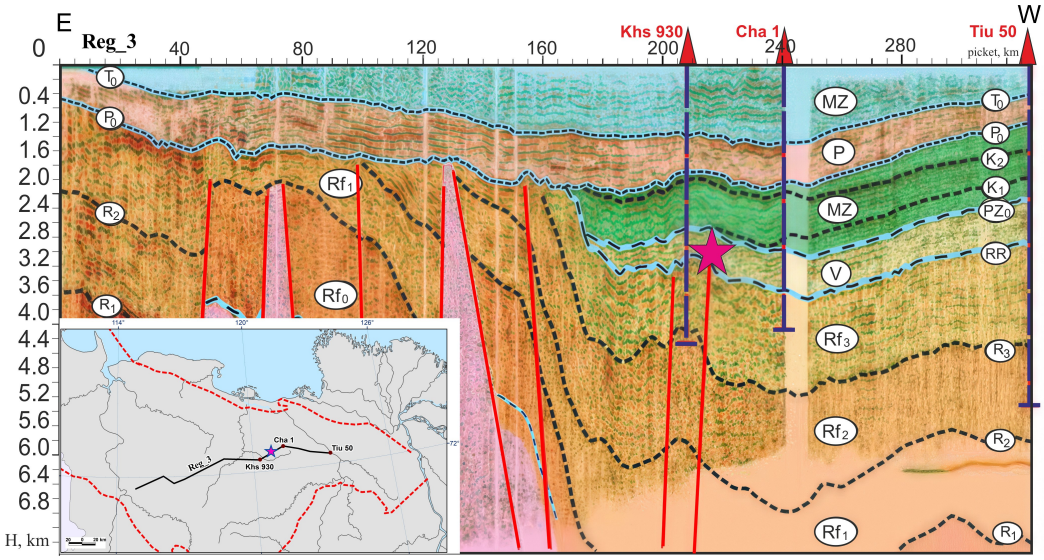

Figure 7. The composite CDP seismic cross-section Reg_3 with interpretation by [*Kontorovich et al.*, 2013]. Red triangles and corresponding blue dashed lines are wells: Khs 930, Khastakh 930; Cha1, Charchikskaya 1; Tiu 50, Tiumyatinskaya 1. Violet star is the Khastakh earthquake source. Position of the Reg_3 profile is shown in the inset.

Therefore, the seismicity distribution, determined primarily by the geodynamic processes, is controlled to a significant extent by structural, compositional, and thermal heterogeneity of the crust, which are reflected in the anomalous geophysical fields. It is widely accepted in the aforementioned papers that rigid blocks with high seismic wave velocities, enhanced resistivity, density, and Poisson's ratios accumulate stresses which could cause ruptures of weakened fault zones and could be dropped in earthquake sources. According to our 3D inversion of the gravity data (Figure 5), the development of the Khastakh seismic event is likely to be controlled by a combination of these factors. The distribution of the magnetic properties of the crust in the source area of the considered event (Figure 4) along with the available geoelectric data (Figure 6) [*Chenborisova*, 2016a,b; *Slinchuk et al.*, 2022] allow us to suggest the relation of the Khastakh earthquake to the boundary of the magmatic body bordered by magma-feeding or magma-controlling fault zones. To sum up, the intrusive body with a positive density contrast and enhanced magnetic properties at its top can be regarded as a concentrator of stresses which could be caused in the study area by a dynamic impact of the areas bordering the Siberian platform [*Imaeva et al.*, 2021]. The focal mechanism of the Khastakh earthquake – almost a pure normal fault formed under the influence of the sub-horizontal SW-NE extension (Figure 1) [*Seredkina and Melnikova*, 2018] – quite agrees with such a hypothesis as the extension with the same orientation dominates in the adjacent areas of the Olenek Bay [*Filippova and Melnikova*, 2023; *Imaeva et al.*, 2017].

Conclusions

To clarify the seismotectonic pattern in the area of the rare May 20, 2011 Khastakh earthquake with M_w = 4.7, occurred on the Siberian platform, spatial characteristics of the gravity and magnetic fields were studied and 3D models of the crustal density and magnetization contrasts were constructed using data on gravity and magnetic surveys [*Buzikova et al.*, 2004; *Lisnik*, 2006] and GIS INTEGRO software [*Cheremisina et al.*, 2021]. The obtained results were compared with the available seismological and geophysical information: earthquake focal mechanism [*Seredkina and Melnikova*, 2018], results of

previous 3D magnetotelluric field inversion [*Slinchuk et al.*, 2022] and the nearest reflection seismic cross-sections [*Kontorovich et al.*, 2013]. The following results were obtained:

1. The buried disjunctives, probably representing fault zones with mineralization development or filled with magmatic material, have been revealed. The epicenter of the Khastakh earthquake has appeared to be coincident with the cross of these structures stretching in sub-latitudinal and NW directions.
2. SW-diping fault plane, associated with the source area of the study seismic event, has been traced based on the results of the 3D spectral inversions of the gravity and magnetic fields. A steep SW-dipping nodal plane is also seen in the previously determined earthquake mechanism. This nodal plane (with strike and dip angles of 105° and 75°, respectively) could be regarded as a rupture plane according to our data.
3. The presence of a magmatic intrusion, probably fed by the inferred magma-controlling fault, is suggested in the vicinity of the Khastakh earthquake source. This intrusive body with a positive density contrast and enhanced magnetic properties at its top can be regarded as a concentrator of stresses which could be caused by a dynamic impact of the areas bordering the Siberian platform, namely, the Olenek Bay.

Therefore, the study has provided insights that the seismicity distribution in the region of Lena-Anabar trough, depending primarily on the geodynamic settings, is also controlled by structural and compositional heterogeneity of the crust. This fact, along with the revealed pattern of the fault network within the area of the Olenek bitumen field, should be taken into account in seismic hazard assessment for the study region in which strategic mineral deposits of the Sakha Republic (Yakutia) are located.

Acknowledgments. The authors are grateful to the colleagues from Nord West Ltd, who provide magnetotelluric materials for the integrated geophysical analyses, as well as colleagues from VNIGNI developing the GIS INTEGRO software. The study was fulfilled under the State Assignments of VNIGNI, IPE RAS, IZMIRAN. The work was carried out with the support of the Ministry of Education and Science of the Russian Federation (within the framework of state assignment No. 075-00604-25) and using data obtained from the unique scientific installation “Seismic infrasound array for monitoring Arctic cryolitozone and continuous seismic monitoring of the Russian Federation, neighbouring territories and the world” (http://www.gsras.ru/unu/).

References

Arefiev S. S., Rogozhin E. A., Aptekman Zh. Ya., et al. Deep structure and tomographic imaging of strong earthquake source zones // Izvestiya, Physics of the Solid Earth. — 2006. — Vol. 42, no. 10. — P. 850–863. — https://doi.org/10.1134/s1069351306100090.

Bukchin B. G. Determination of source parameters from surface wave recording allowing for uncertainties in the properties of the medium // Izvestiya, Physics of the Solid Earth. — 1990. — Vol. 25. — P. 723–728.

Buzikova O. G., Lisnik G. A., Kovaleva N. P., et al. Creation of a digital map of the gravity field of the territory of the Republic of Sakha (Yakutia) at the scales of 1:500,000, 1:1,000,000, 1:1,500,000, 1:2,500,000, 1:5,000,000 as of 1.01.2005, in 2002-2004: geological report. — Yakutsk : Rosgeolfond, 2004. — (In Russian).

Chenborisova R. Z. Report on the results of work on the object 81-97 "Carrying out complex field geophysical works to prepare new zones of oil and gas accumulation in the Anabar-Laptev region". Registration number 3014849. — TsentrSibnedra JSC "Rosgeologiya", 2016a. — (In Russian).

Chenborisova R. Z. Report on the results of work on the object 81-99 "Carrying out complex field geophysical works to identify new zones of oil and gas accumulation in the zone of conjunction of the Yenisei-Khatanga and Lena-Anabar troughs (Severo-Anabar area)". Registration number 3014854. — TsentrSibnedra JSC "Rosgeologiya", 2016b. — (In Russian).

Cheremisina E. N., Finkel’shtein M. Ya., Deev K. V., et al. GIS INTEGRO. Status and prospects for development in the context of import substitution // Geologiya nefti i gaza. — 2021. — No. 3. — P. 31–40. — https://doi.org/10.31087/0016-7894-2021-3-31-40. — (In Russian).

Dong C., Chen B. and Wang C. Magnetic Anomaly Characteristics and Magnetic Basement Structure in Earthquake-Affected Changning Area of Southern Sichuan Basin, China: A New Perspective from Land-Based Stations // Remote Sensing. — 2022. — Vol. 15, no. 1. — P. 23. — https://doi.org/10.3390/rs15010023.

Filippova A. I. and Filippov S. V. Depth to the Bottom of Lithospheric Magnetic Sources Beneath Northeastern Eurasia: Lithospheric Thermal Regime and Relation to Seismicity // Geomagnetism and Aeronomy. — 2024. — Vol. 64, no. 1. — P. 128–137. — https://doi.org/10.1134/S0016793223600790.

Filippova A. I. and Melnikova V. I. Crustal Stresses in the East Arctic Region From New Data on Earthquake Focal Mechanisms // Tectonics. — 2023. — Vol. 42, no. 9. — e2022TC007338. — https://doi.org/10.1029/2022tc007338.

Gou T., Zhao D., Huang Z., et al. Structural Heterogeneity in Source Zones of the 2018 Anchorage Intraslab Earthquake and the 1964 Alaska Megathrust Earthquake // Geochemistry, Geophysics, Geosystems. — 2020. — Vol. 21, no. 3. — e2019GC008812. — https://doi.org/10.1029/2019gc008812.

Imaeva L., Gusev G., Imaev V., et al. Neotectonic activity and parameters of seismotectonic deformations of seismic belts in Northeast Asia // Journal of Asian Earth Sciences. — 2017. — Vol. 148. — P. 254–264. — https://doi.org/10.1016/j.jseaes.2017.09.007.

Imaeva L. P., Mackey K. G., Koz'min B. M., et al. Seismotectonic reactivation marginal suture zones of the Siberian craton // Arctic and Subarctic Natural Resources. — 2021. — Vol. 26, no. 2. — P. 7–26. — https://doi.org/10.31242/2618-9712-2021-26-2-1. — (In Russian).

Kayal J. R., Zhao D., Mishra O. P., et al. The 2001 Bhuj earthquake: Tomographic evidence for fluids at the hypocenter and its implications for rupture nucleation // Geophysical Research Letters. — 2002. — Vol. 29, no. 24. — P. 2152–2152. — https://doi.org/10.1029/2002gl015177.

Khudoley A. K., Frolov S. V., Akhmanov G. G., et al. Anabar-Lena Composite Tectono-Sedimentary Element, northern East Siberia // Geological Society, London, Memoirs. — 2022. — Vol. 57, no. 1. — https://doi.org/10.1144/m57-2021-29.

Kim C. H., Kim K. H., Choi S. Y., et al. Gravity and magnetic anomalies of earthquake-prone areas in the southwestern Ulleung basin margin, East Sea (Sea of Japan) // Scientific Reports. — 2022. — Vol. 12, no. 1. — P. 1–16. — https://doi.org/10.1038/s41598-022-21462-3.

Kobrunov A. I. and Varfolomeev V. A. One approach of density equivalent representation and using it for gravity field interpretation // Earth Physics USSR Academy of Science. — 1981. — No. 10. — P. 25–44. — (In Russian).

Kontorovich V. A., Kontorovich A. E., Gubin I. A., et al. The Neoproterozoic-Phanerozoic section of the Anabar-Lena province: structural framework, geological model, and petroleum potential // Russian Geology and Geophysics. — 2013. — Vol. 54, no. 8. — P. 980–996. — https://doi.org/10.1016/j.rgg.2013.07.014.

Kopnichev Yu. F. and Sokolova I. N. Spatiotemporal Variations of the S Wave Attenuation Field in the Source Zones of Large Earthquakes in the Tien Shan // Izvestiya, Physics of the Solid Earth. — 2003. — Vol. 39, no. 7. — P. 568–579.

Krylov S. V. and Ten E. N. Strength and Elastic Properties of Focal Zones of Violent Earthquakes within the Baikalian and North Tien Shan Areas // Geologiya i Geofizika. — 1995. — Vol. 36, no. 2. — P. 137–150. — (In Russian).

Kulyandina A. S., Sokolova E. Yu. and Filippova A. I. Analysis of relation between seismicity and features of potential fields within the Lena-Anabar trough: experience of usage modern GIS-technologies // Geoinformatika. — 2024. — No. 2. — P. 12–24. — https://doi.org/10.47148/1609-364X-2024-2-12-24. — (In Russian).

Lisnik G. A. Creation of a digital map of the anomalous magnetic field (ΔTa) of the territory of the Republic of Sakha (Yakutia) on a scale of 1:500,000, 1:1,500,000, 1:5,000,000 as of 01.01.2005 in 2003-2006 : explanatory letter. — Yakutsk : Rosgeolfond, 2006. — (In Russian).

Mitsyn S. V. On Numeric Implementation of Spectral Method of Gravimetry Inverse Problem // Geoinformatika. — 2018. — No. 3. — P. 89–97. — (In Russian).

Priezzhev I. Spectral and statistical analyses of aero geophysical data in system ASOM-AGS/ES : PhD thesis / Priezzhev I. — 1989. — (In Russian).

Priezzhev I., Scollard A. and Lu Z. Regional production prediction technology based on gravity and magnetic data from the Eagle Ford formation, Texas, USA // SEG Technical Program Expanded Abstracts 2014. — Society of Exploration Geophysicists, 2014. — P. 1354–1358. — https://doi.org/10.1190/segam2014-0289.1.

Radziminovich Y. B. and Shchetnikov A. A. Historical seismicity on the southern margin of the Siberian craton: new data // Russian Geology and Geophysics. — 2008. — Vol. 49, no. 9. — P. 698–707. — https://doi.org/10.1016/j.rgg.2007.12.013.

Rautian T. G., Khalturin V. I., Fujita K., et al. Origins and Methodology of the Russian Energy K-Class System and Its Relationship to Magnitude Scales // Seismological Research Letters. — 2007. — Vol. 78, no. 6. — P. 579–590. — https://doi.org/10.1785/gssrl.78.6.579.

Seminskii K. Z. and Radziminovich Y. B. Seismicity of the southern Siberian platform: Spatiotemporal characteristics and genesis // Izvestiya, Physics of the Solid Earth. — 2007. — Vol. 43, no. 9. — P. 726–737. — https://doi.org/10.1134/s1069351307090029.

Seredkina A., Melnikova V., Gileva N., et al. The Mw 4.3 January 17, 2014, earthquake: very rare seismic event on the Siberian platform // Journal of Seismology. — 2015. — Vol. 19, no. 3. — P. 685–694. — https://doi.org/10.1007/s10950-015-9487-y.

Seredkina A. I. and Melnikova V. I. New data on earthquake focal mechanisms in the Laptev Sea region of the Arctic-Asian seismic belt // Journal of Seismology. — 2018. — Vol. 22, no. 5. — P. 1211–1224. — https://doi.org/10.1007/s10950-018-9762-9.

Slinchuk G. E., Yakovlev D. V., Yakovlev A. G., et al. Geoelectrical Model of the Deep Structure of the Yenisei-Khatanga Regional Trough // Izvestiya, Physics of the Solid Earth. — 2022. — Vol. 58, no. 5. — P. 655–669. — https://doi.org/10.1134/s1069351322050123.

Sokolova E., Berdichevsky M., Varentsov I., et al. Advanced methods for joint MT/MV profile studies of active orogens: The experience from the Central Tien Shan // Proc. Colloquium Electromagnetic Depth Research, 22nd, Děčín, Czech Republic. — Potsdam, Germany : Deutsche Geophysikalische Gesellschaft, 2007. — P. 132–141.

Sokolova E. Yu., Israil M., Gupta P., et al. Crustal electrical conductivity of the Indian continental subduction zone: New data from the profile in the Garhwal Himalaya // Izvestiya, Physics of the Solid Earth. — 2016. — Vol. 52, no. 2. — P. 271–290. — https://doi.org/10.1134/s1069351316020130.

Unsworth M. J. Magnetotelluric Studies of Active Continent-Continent Collisions // Surveys in Geophysics. — 2009. — Vol. 31, no. 2. — P. 137–161. — https://doi.org/10.1007/s10712-009-9086-y.

Wei W. and Zhao D. Tomography of the source zone of the 2015 M 7.8 Nepal earthquake // Physics of the Earth and Planetary Interiors. — 2016. — Vol. 253. — P. 58–63. — https://doi.org/10.1016/j.pepi.2016.01.008.

Wen L. M., Kang G. F., Bai C. H., et al. Relationship between crustal magnetic anomalies and strong earthquake activity in the south segment of the China North-South Seismic Belt // Applied Geophysics. — 2021. — Vol. 18, no. 3. — P. 408–419. — https://doi.org/10.1007/s11770-021-0870-x.

Wu G., Tan H., Yang G., et al. Research on the relationship between geophysical structural features and earthquakes in Mid-Yunnan and the surrounding area // Geodesy and Geodynamics. — 2015. — Vol. 6, no. 5. — P. 384–391. — https://doi.org/10.1016/j.geog.2015.07.003.

Yang H., Xiong Z., Liu Q., et al. The crustal structure of the Longmenshan fault zone and its implications for seismogenesis: new insight from aeromagnetic and gravity data // Solid Earth. — 2023. — Vol. 14, no. 12. — P. 1289–1308. — https://doi.org/10.5194/se-14-1289-2023.

Zhang J., Gao R., Zheng L., et al. Relationship between characteristics of gravity and magnetic anomalies and the earthquakes in the Longmenshan range and adjacent areas // Tectonophysics. — 2010. — Vol. 491, no. 1–4. — P. 218–229. — https://doi.org/10.1016/j.tecto.2009.12.004.